

REMARKS/ARGUMENTS

**Rejection of claims 1, 5, 13 and 16-21 under 35 U.S.C 103(a) as being
unpatentable over Applicant's admitted prior art (APA), figures 1-2, in view of
5 Sato, US 2006/0097380.**

Applicants respectfully submit a document titled "Measurements of Time-Dependent
Mura in LCD Manufacture" as attached in the appendix for investigating the
phenomenon of curtain mura in COG technique.

10

As discussed in the attached document, one of the major problems in COG (chip on
glass) interconnection is curtain mura, which is a periodical bright and dark
phenomenon near the peripheral of TFT-LCD. Figure 1 is a typical configuration of
curtain mura, and the resolution of display is XGA and the active area is 15 inch.

15 COG drivers are attached on top (source) and left (gate) side of display and it has been
found that both source and gate sides have the light leakage problem under and
between COG drivers.

The root cause of curtain mura is residual stress between glass and drivers after COG
20 bonding. The residual stress will bend the glass and influence the cell gap of LCDs.
There are many factors affecting the warpage of glass in COG, including the fillets in
ACF (anisotropic conductive film). In our investigation, the ACF curing parameters,
driver and glass thickness also play an important role in the warpage of LCDs. The
thinner of glass design in LCD display, the more serious of curtain mura will be.

25 The applicants also found that not only COG but also COF and TAB module have the
same issue when using 48mm width tape carrier.

In order to resolve the aforementioned curtain mura issue, claims 1 and 13 have been
further amended to specify that the thickness of the driver chips (such as the gate
30 driver chip and the source driver chip) is less than 0.15 mm. As the semiconductor

module taught by Sato belongs to a completely different field from the LCD module of the present invention and clearly fails to explicitly teach that the thickness of the chip is thinned to reduce the issue of curtain mura pertaining to a LCD module, applicants submit that the two prior arts cannot be combined in the manner suggested and the LCD module of the present invention is patentable over the two cited references. Reconsideration of amended claims 1 and 13 is respectfully requested. As claims 5 and 16-21 are dependent upon claims 1 and 13, applicants submit that if claims 1 and 13 are found allowable, claims 5 and 16-21 should additionally be found allowable.

Applicant respectfully requests that a timely Notice of Allowance be issued in this case.

Sincerely yours,

/Winston Hsu/

Date: 08/14/2009

Winston Hsu, Patent Agent No. 41,526

P.O. BOX 506, Merrifield, VA 22116, U.S.A.

Voice Mail: 302-729-1562

Facsimile: 806-498-6673

e-mail : winstonhsu@naipo.com

Note: Please leave a message in my voice mail if you need to talk to me. (The time in D.C. is 12 hours behind the Taiwan time, i.e. 9 AM in D.C. = 9 PM in Taiwan.)

Paper Title

Measurements of Time-Dependent Mura in LCD Manufacture

Pao-Yun Tang, Kei-Hsiung Yang*, Shu-lin Ho*, Chen-Han Kuo**, Zih-Jian Jhang**, Kai-Chieh Chang***

*Hannstar, Taoyuan 326, Taiwan.

**TTLA, Taiwan TFT LCD Association, Hsinchu 310, Taiwan.

Abstract

After chip-on-glass process on TFT-LCD panels, we have observed the occurrence of curtain mura and it has varied as the panel ages. In this paper, we used novel methods to measure and analyze this phenomenon of mura aging, including intensity profile, contrast profile, local contrast profile and just-noticeable-difference (JND) profile. Results revealed that the JND profile of some muras decayed day by day, but their areas and shapes maintained roughly the same. In addition, a subjective experiment was conducted to find the human eyes' contrast threshold of curtain mura. Finally, our methods can be used to reduce testing time to validate the robustness of the display, and establish accelerated measuring techniques to find the corrosion failure

Presentation Style

Poster.

Workshop

VHF.

1. Introduction

COG (Chip on Glass) is a popular technology in small and medium size liquid crystal displays (LCDs), partially because the cost of driver is higher than panel, the recycle of LCD panel is not so important. For notebook and monitor LCDs, the pixel control devices are made of thin film transistors (TFTs) and the cost of panel is higher than driver. The yield and reliability are the major concern for the selection of COG technology. Tape automated bonding (TAB) and Chip-on Flex (COF) technologies are the best choice for large size TFT-LCDs module package. As the pixel density increasing, the OLB (outer lead bonding) pitch of TAB and COF become small which will make a limitation on the production of tape carrier and LCM (LCDs module). The fine pitch (under 50 μm) of COF and TAB has the drawbacks of micro cracks and breaking problem on copper trace during module assembly process (especially for those drivers locate at the corner of display). To improve the reliability of LCM, most of LCM makers begin to study the possibility of manufacturing large size LCM by COG technology.

Recently, the high yield of drivers and improvement of COG repair methodology make the multi-chips COG interconnection become a valuable technology in large size TFT-LCDs applications.

2. Formation of Time-Dependent Mura

One of the major problems in COG interconnection is curtain mura which is a periodical bright and dark phenomenon near the peripheral of TFT-LCD. Figure 1 is the typical configuration of curtain mura. The resolution of display is XGA and the active area is 15 inch. COG drivers are attached on top (source) and left (gate) side of display. We can find both source and gate sides have the light leakage problem under and between COG drivers.

The root cause of curtain mura is residual stress between glass and drivers after COG bonding. The residual stress will bend the glass and influence the cell gap of LCDs. There are many factors that will affect the warpage of glass in COG, including the fillets in ACF [1]. In our investigation, the ACF (anisotropic conductive film) curing parameters, driver and glass thickness also play an important role in the warpage of LCDs. The thinner of glass design in LCD display, the more serious of curtain mura will be. Besides, we also find that not only COG but also COF and TAB module have the same issue when we use 48mm width tape carrier.

Curtain mura can be observed at the dark state of display and it will change by different view angle. The mechanism of curtain mura needs more investigation and we believe this phenomenon has relationship with the properties of liquid crystal. The aging test of LCM can reduce the curtain mura to certain degree, but we can't eliminate this phenomenon by temperature cycling only, because most of the stress will recover when the temperature is cooling down.

There will also be a problem on the selection of limit sample, a standard between LCD vender and customer to judge the quality of image after mass-production, because the curtain mura will reduce during storage. We have to study the standardization of curtain mura by image processor, not by limit sample.

3. Experiments

3.1 Experiment conditions

In our experiment, MegaPlus II ES4020 camera from REDLAKE with 4M pixel CCD was utilized to gather images of LCD panels of bottom view at Inclination $\theta_V = -25^\circ$. Fig. 2 shows an example of result images. Observing distance is 1.4M from camera CCD to LCD panel and capturing was processed under dark-room environment with 92 gray-level pattern. The target panel is 15 inch with XGA resolution and bounding by COG driver.

3.2 Test procedures

To observe the transformation of captured mura images and to find an effective index measuring the phenomena of time-dependent mura, we performed various algorithms including intensity profile, global contrast, local contrast and mura JND values calculation.

In the analysis, we first defined a target section in image where horizontally crosses pairs of adjacent bright and dark areas. In intensity profile, we calculated difference of certain selected part in defined pairs. In global (Fig. 4) and local contrast (Fig. 5) profiles, analysis was performed with gray-level contrasts of the serial data images in predefined regions by global and local backgrounds. Also, in JND contrast profile (Fig. 6), we obtained mura JND values by structured Human Vision Model [5], which defines responses of mura images corresponding to human factor vision perception. From the result profiles of mentioned algorithms, an addition PCA (Principle Component Analysis) fitting analysis (Fig. 7) was operated to verify that whether the areas and shapes of muras in measuring times differ or not.

3.3 Subjective experiments

For comparing with the performance between the capturing system and human eyes, we briefly conducted a two factor factorial analysis of variances with repeated measurements. The independent variables were visual angles (VA) of curtain mura and subjects. The size of all mura stimulus were fixed in X-direction, VA was 5.75° . The levels of VA were 1.05° , 2.14° , 4.33° , 8.69° and 17.27° in Y-direction respectively. Five stimulus are shown in Fig. 8.

The dependent variable, the contrast threshold was obtained from two-alternative forced choice method. All experiment conditions and apparatus were similar to the previous study [5]. The results of the ANOVA are summarized in Table 1. The total sum of squares is 1526.76 and by subtraction 724.45. Table * confirmed the significance of the VA effects. The main effects of VA were significant on contrast thresholds: 11.69 compared with $F(0.01, 4, 51)=3.74$.

We can conclude that there are significant differences among the contrast thresholds of the five visual angles. The contrast threshold results illustrated in Fig. 9 are the average contrast thresholds of the five visual angles. From these results, it can be seen that larger VA would bring about lower contrast threshold. In addition, we found that the average of contrast threshold was around -19.1051 dB for 8.69° VA which was the initial size of curtain mura in TFT-LCD modules for major desktop applications.

4. Results and Discussion

The main process procedure is shown in Fig.11. Figure 3, 4, 5 and 6 are the corresponding results of intensity profile, global contrast, local contrast and JND profile. In the first three measuring algorithms, we hardly find the transformation trend of muras from serial images. However, the corresponding peak JND index profile represents a decay curve of the mura which matches the human vision perception. The result of PCA fitting in Fig.7 shows the constancy of muras in area and shape making first three indexes more ineffective. The subjective experiment result of human eyes' contrast threshold in curtain mura describes curtain mura-less period of JND values. Accordingly, we could sketch a decay curve of mura peak JND value in time domain, Fig. 10, and it defines the transformation trend of curtain mura in time period.

5. Conclusions

During a period of time, we observed COG panels with time-dependent mura. By the calculated peak JND index profile as well as the human eyes' contrast threshold in curtain mura, we defined peak JND decay curve of the corresponding time-dependent mura. From the studied results we could not only reduce testing time to validate the robustness of the display but also establish acceleration measuring techniques to rapidly induce the corrosion failure. Moreover, the proposed predictive decay curve could be improved by adopting more samples with similar structure to the target.

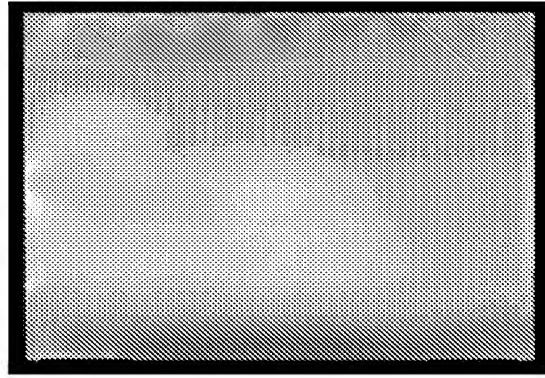


Fig. 1. Configuration of COG curtain mura

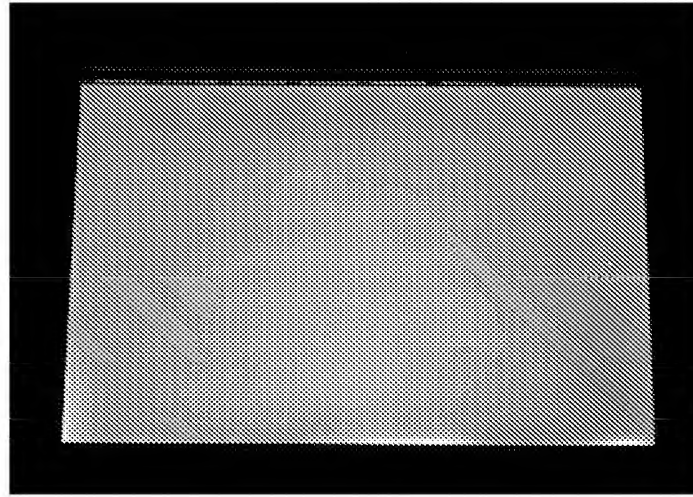


Fig. 2. Captured LCD image from bottom view

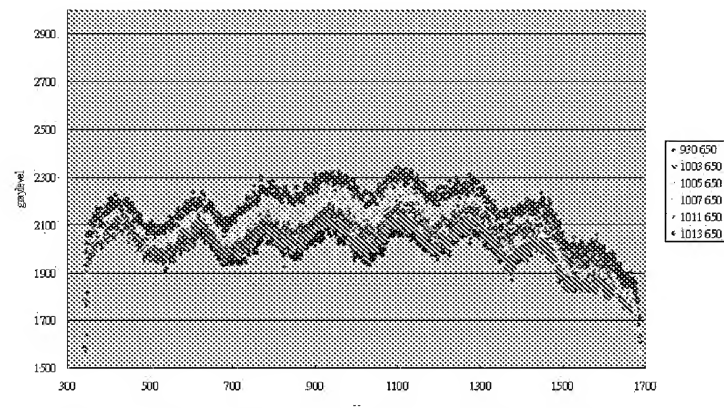


Fig. 3. Gray-level profile in X-direction and colors represent different measuring time slots.

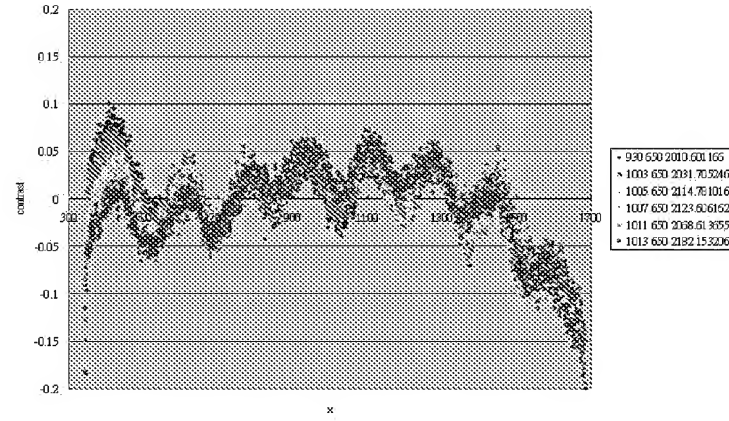


Fig. 4. Global contrast profile in X-direction and colors represent different measuring time slots.

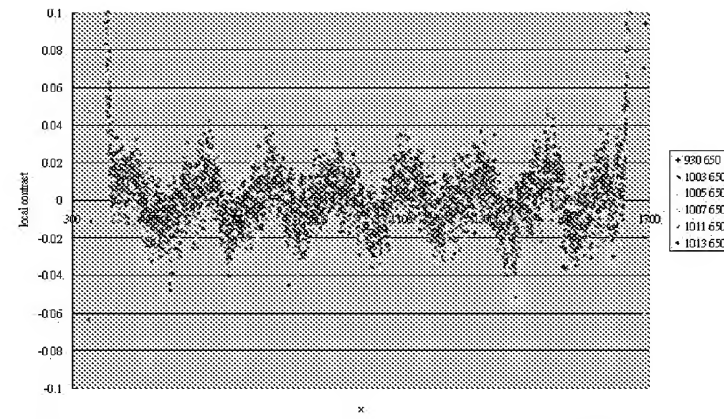


Fig. 5. Local contrast profile in X-direction and colors represent different measuring time slots.

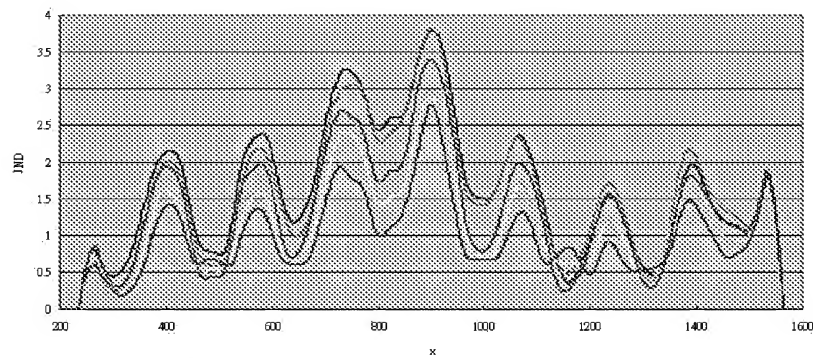


Fig. 6. JND profile in X-direction and colors represent different measuring time slots.

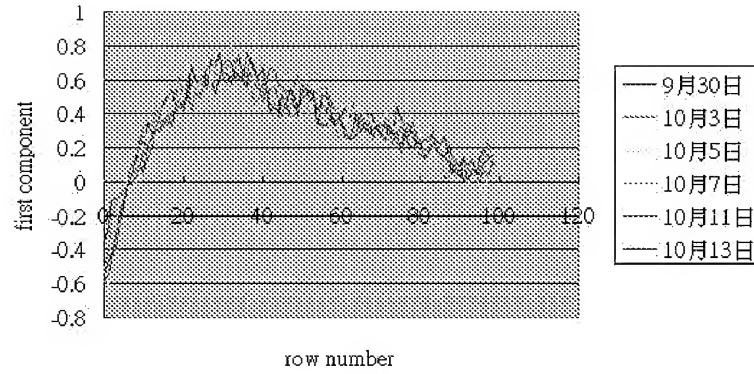


Fig. 7. Result of PCA fitting analysis in mura area and shapes.

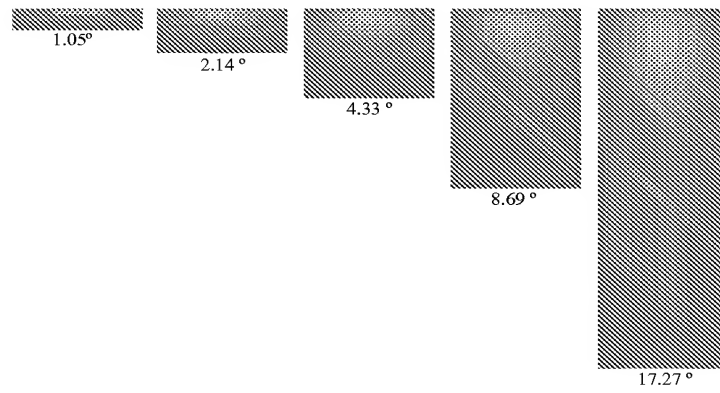


Fig. 8. Five stimulus of curtain mura in subjective experiments

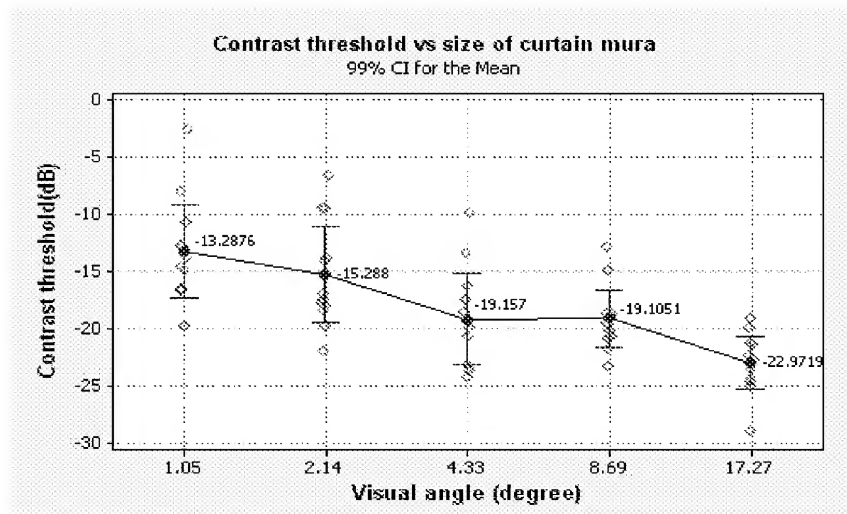


Fig. 9. Means of the contrast thresholds for each visual angles (error bars represent 99% confidence intervals)

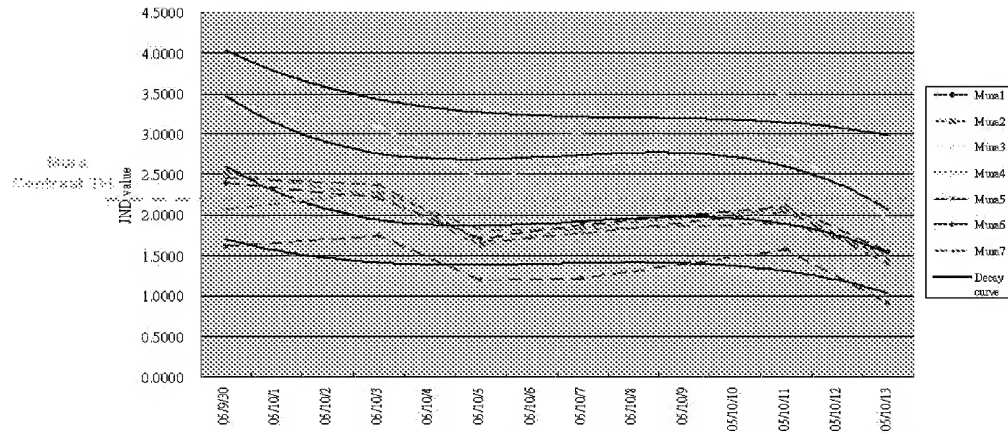


Fig. 10. Peak JND values of measured mura and calculated decay curve. Colors represent different mura positions.

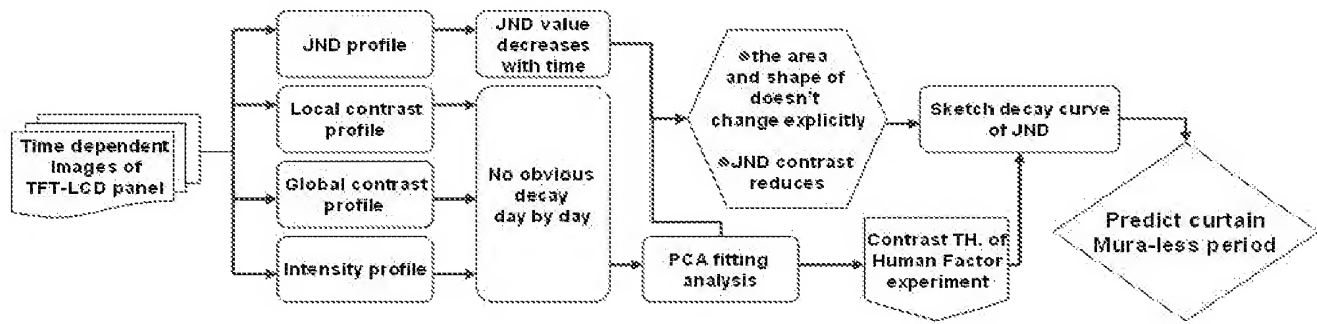


Fig. 11. Main concept procedure of Time-dependent mura analysis.

Table 1. Analysis of Variance for Contrast Threshold of Curtain Mura

Source of variance	Degree of freedom	Sum of squares	Adjust sum of square	Adjust mean square	F ₀	P
Subject	4	120.31	120.31	30.08	2.12	0.092
VA	4	682	664.47	170.5	11.69*	0.000
Error	51	724.45	724.45	14.2		
Total		1526.76				

*Significant at 1 percent

Reference

1. M. Y. Tsai, C.Y. Wu, C.W. Huang, W.C. Cheng, S.R. Kang, S.S. Yang and S.M. Chang, "Effects of Some Parameters on Warpage and Bump-Joint Stress of COG Packages", Proceedings of 4th IEEE International Conference on Polymers and Adhesives in Microelectronics and Photonics, Polytronic 2004, pp182-190, 2004.
2. Kouichi Murakoshi, Jyunichi Kanazawa and Shigeyuki Ogata, "The factors influencing environmental reliability of chip-on-glass technology," IEEE/CHMT '89 Japan IEMT Symposium, pp342-349, 1989.
3. A. Schubert, R Dudek, R. Diiring, and B. Michel, "Reliability Investigations of Flip Chip Interconnects in FCOB and FCOG Applications by FEA," 1998 IEEE/CPMT Electronics Packaging Technology Conferenc, pp49-56, 1998.
4. Bin Xie and Han Ding, "New challenges in design and understanding of chip-on-glass (COG) for LCD packaging by

- FEA,” Proceedings of 2005 International Conference on Asian Green Electronics, pp79-85, 2005.
5. S.B. Wang, Z.J. Jhang, C.H. Wen, “A mura matric based on human vision models,” SID06, 2006.